

# TECHNICAL DESIGN GUIDE FOR TIMBER-CONCRETE COMPOSITE FLOORS – A CANADIAN APPROACH

Samuel Cuerrier Auclair<sup>1</sup>, Christian Dagenais<sup>2</sup>, Sylvain Gagnon<sup>3</sup>

**ABSTRACT:** FPInnovations, a not-for-profit research organisation for the Canadian forest sector and affiliated industries, developed a technical design guide for timber-concrete composite (TCC) floors meeting multi-design requirements. It provides the design criteria along with the calculation methods to control the elastic and long-term deflection, the vibration induced by human walking and the structural resistance, as well as guidance for the fire-resistance design and the behaviour of the shear connection. The technical guide has been used to develop design provisions that are expected to be implemented in the next 2024 edition of CSA O86. This paper presents a summary of this Canadian design method.

**KEYWORDS:** Timber-concrete composite (TCC), multi-criteria design, floor vibration, fire resistance, shear connector

## 1 INTRODUCTION

A timber-concrete composite (TCC) system consists of two distinct layers, a timber layer and a concrete layer, joined together by shear connectors; typically, the concrete slab is the top layer. The properties of both materials are better exploited as a composite element, since tension forces from bending are mainly resisted by the timber while compression forces from bending are resisted by the concrete. This construction technique is used to strengthen and stiffen timber floors of existing and new constructions, especially in multi-storey buildings and long-span applications. When the two materials are well connected together, the load-carrying capacity and the bending stiffness are significantly increased compared to a traditional timber floor system [1]. The concrete layer is usually a reinforced concrete slab. The timber part can be solid wood lumber, glued laminated timber (Glulam), structural composite lumber (SCL), cross-laminated timber (CLT), nail-laminated timber (NLT) or made of other engineered wood products. The shear connectors can be discrete fasteners (e.g., nails, screws, or notches cut in the wooden part) or shear connectors transferring the load to a larger surface (e.g., embedded plates, glue). A combination of different shear connectors is also possible.

The development of the TCC system was initiated after the First World War to find an alternative for reinforced concrete and steel, because of a lack of availability of steel. Several connection systems were patented [2, 3]. In the 1930's, this construction technique was applied to bridges mainly located in the U.S.A. [4]. In the 1950's, TCC building structures appeared in Australia and New Zealand [5]. It was ignored in most parts of the world until the 1990's, when TCC structures started to be used when

refurbishing old historical buildings in European cities, in order to meet the new requirements regarding sound insulation and fire-resistance [6].

TCC systems can be a cost-competitive solution in the construction of buildings with floors having longer spans, since the mechanical properties of the two materials would be used efficiently. Furthermore, the additional mass from the concrete can improve the acoustic performance, compared to that of a timber floor system alone. Nevertheless, TCC floors are not commonly used in buildings in Canada, due to the absence of technical guidelines in the Canadian wood engineering design standard CSA O86-19 [7].

## 2 OBJECTIVES

The objectives of this paper are to present the multi-criteria design guide for TCC floors in Canada written by FPInnovations [8]. The criteria considered in the design are:

- 1) the elastic and the long-term deflections,
- 2) the vibration performance due to human normal walking,
- 3) the ultimate limit state design (bending and shear resistance) and,
- 4) the structural fire resistance.

The methodology used to verify those criteria are based on the gamma-method ( $\gamma$ -method) which was developed by Möhler [9] in 1956 by applying a sinusoidal load on a composite beam.

<sup>1</sup> Samuel Cuerrier Auclair, FPInnovations, Canada, samuel.cuerrier-auclair@fpinnovations.ca

<sup>2</sup> Christian Dagenais, FPInnovations, Canada, christian.dagenais@fpinnovations.ca

<sup>3</sup> Sylvain Gagnon, FPInnovations, Canada, sylvain.gagnon@fpinnovations.ca

### 3 EVALUATION OF THE EFFECTIVE BENDING STIFFNESS

Using the  $\gamma$ -method, available in Annex B of the Eurocode 5 [10], the effective bending stiffness of the composite system can be evaluated. The  $\gamma$ -method assumes a uniformly distributed shear stiffness,  $K$ , between the two connected components, being timber and concrete. If the spacing of the shear connector is not constant along the span, an effective spacing needs to be estimated as follows:

$$s_{eff} = 0.75s_{min} + 0.25s_{max} \quad (1)$$

where  $s_{min}$  is the spacing of the shear connector near the supports in mm and  $s_{max}$  is the connector spacing in the mid-span section in mm. The uniformly distributed shear stiffness is then calculated as follows:

$$K = \frac{nk}{s_{eff}} \quad (2)$$

where  $n$  is the number of rows of the shear connectors and  $k$  is stiffness of a single shear connector in N/mm.

The tension contribution of the concrete must be neglected to be in-line with the concrete design standard in Canada (CSA A23.3) [11]. Figure 1 shows the nomenclature used and the cross-section with the associated axial deformation used for the calculation.

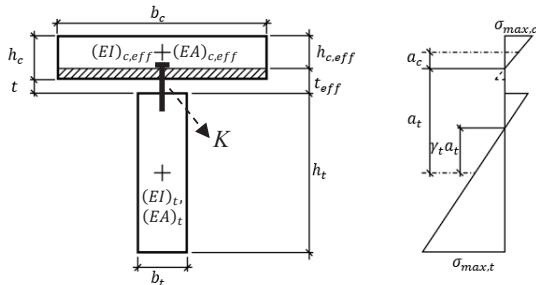


**Figure 1:** Cross-section and axial deformation of a TCC beam neglecting the concrete solicited in tension

$$(EI)_{eff} = (EI)_{c,eff} + (EI)_{t,eff} + \gamma_c(EA)_c\alpha_c^2 + \gamma_t(EA)_t\alpha_t^2 \quad (3)$$

Where,

$$\gamma_c = 1 \text{ and } \gamma_t = \frac{1}{1 + \frac{\pi^2(EA)_t}{KL^2}} \quad (4)$$

$$h_{c,eff} = \min(\sqrt{\alpha^2 + \alpha(h_t + 2h_c + 2t)} - \alpha; h_c) \quad (5)$$

$$\alpha = \frac{\gamma_t(EA)_t}{E_c b_c} \quad (6)$$

$$(EA)_{c,eff} = E_c b_c h_{c,eff} \text{ and } (EI)_{c,eff} = \frac{E_c b_c h_{c,eff}^3}{12} \quad (7)$$

$$a_c = \frac{\gamma_t(EA)_t r}{(EA)_{c,eff} + \gamma_t(EA)_t} \text{ and } a_t = r - a_c \quad (8)$$

$$r = \frac{h_t}{2} + t + h_c - \frac{h_{c,eff}}{2} \quad (9)$$

Where  $(EI)_{eff}$  is the effective bending stiffness in N-mm<sup>2</sup>.  $(EI)_{c,eff}$  and  $(EA)_{c,eff}$  are the effective bending stiffness and the axial stiffness of the concrete slab by neglecting the portion in concrete in N-mm<sup>2</sup> and in N, respectively.  $(EI)_t$  and  $(EA)_t$  are the bending stiffness and the axial stiffness of the timber component in N-mm<sup>2</sup> and in N, respectively.  $\gamma_c$  and  $\gamma_t$  are the composite factor of the concrete and wood component, respectively.  $E_c$ ,  $b_c$  and  $h_c$  are the modulus of elasticity, the effective width and the thickness of the concrete slab in MPa, mm and mm, respectively.  $h_t$  is the height of the wood component in mm.  $a_c$  and  $a_t$  are the distance between the centroid of the concrete slab and the timber to the neutral axis of the concrete slab in mm, respectively.  $L$  is the span of the TCC floor in mm.  $t$  is the gap between the concrete slab and the timber component in mm.  $r$  is the distance between the centroids of the concrete slab and the wood component in mm.

### 4 SHEAR CONNECTION PROPERTIES

The type of shear connection between the timber and concrete components greatly influences the structural properties of TCC floors. A wide range of connection systems are available, ranging from mechanical connectors such as bolts [12], lag screws [13], or self-tapping screws (STS) [14], glued-in perforated steel plates [15], composite connectors [16], adhesive bonds [17], notched connections [18], or steel kerf plates [19].

When possible, the shear resistance of the shear connector should be estimated with the appropriate Clause 12 in CSA O86-19 [7]. When not possible, the shear resistance needs to be estimated through laboratory testing.

CSA O86-19 [7] does not give equation to estimate the slip modulus of connectors. Thus, this property needs to be evaluated in a laboratory. The testing need to be performed in accordance with the standard ISO 6891 [20].

### 5 ELASTIC AND LONG-TERM DEFLECTIONS

#### 5.1 ELASTIC DEFLECTIONS

In Canada, the deflection limit for timber structure under serviceability loads are prescribed by CSA O86-19 [7]. Estimating the elastic deflection is relatively straightforward, the effective bending stiffness is estimated using the standard-term properties of each

material and using the serviceability limit state slips modulus of the shear connector. Once this, effective bending stiffness is estimated, the instantaneous deflection can be estimated with the serviceability load combination considered.

## 5.2 LONG-TERM DEFLECTION

The long-term deflection is estimated by the superimposition principles. Two portions of the total deflection can be defined:

- 1) the elastic deflection due to transient load evaluated with the previous subsection and
- 2) the long-term deflection, which includes the elastic and creep portion, due to quasi-permanent and permanent loads.

The second portion is evaluated by dividing the stiffness properties of each material (e.g., timber, concrete and shear connector) by their respective creep modification factors. Creep modification factors are numerically equivalent to the creep coefficient by adding 1 to the value. Once the stiffness of each material is modified, the long-term effective bending stiffness can be estimated to calculate the long-term deflection due to quasi-permanent and permanent loads.

## 6 VIBRATION PERFORMANCE DUE TO WALKING

Human normal walking excites the floor through its footstep. Significant efforts were made towards understanding the nature of footsteps [21-24]. Based on their findings, it can be concluded that the footstep force generated by walking comprises two components [22]. One component is a short duration impact force induced by the heel of each footstep on the floor surface where the duration of the heel impact varies from about 30 ms to 100 ms depending on the conditions and the materials of the two contact surfaces (that of the floor and the footwear of the walking person), and on the weight and gait of the person. The other component is the walking rate, a series of footsteps consisting of a wave train of harmonics, at multiples of about 2 Hz.

To understand how TCC floors behave under walking vibration, FPInnovations tested three different laboratory floors:

- 1- NLT-concrete composite slab floor with a nail plate as shear connectors;
- 2- CLT-concrete composite slab floor with self-tapping screws as shear connectors;
- 3- Concrete slab - glulam beams composite floor with self-tapping screws as shear connectors.

The three floors have been tested according to the ISO 18324 [25] and ISO 21136 [26] in order to evaluate their natural frequency, damping ratio, static deflection under a concentrated load and their vibration performance under a subjective evaluation. From these tests, design criteria to limit the span due to vibration induce by walking has

been developed. More information on the tested laboratory TCC floors can be found in [27].

Using the subjective evaluation results of the three tested TCC floor along with their calculated natural frequencies and deflections, the following design criterion was derived using the method described in ISO 21136 [26].

$$\frac{f_1}{d_{1kN}^{0.14}} \geq 5.75 \quad (10)$$

where  $f_1$  is the fundamental natural frequency in Hz and  $d_{1kN}$  is the static deflection under a 1 kN point load in mm. Assuming a simple span floor with a centre point load, Equation (10) can be rewritten as follows to limit the span.

$$L \leq 0.329 \frac{((EI)_{eff}^{1m})^{0.264}}{m_L^{0.207}} \quad (11)$$

where  $L$  is the maximum allowable clear span in meter for the vibration criterion.  $(EI)_{eff}^{1m}$  is the effective bending stiffness of the floor calculated with Equations (3) considering the standard-term material properties for 1-meter-wide floor in N-m<sup>2</sup> and  $m_L$  is the structural mass only of the 1-meter-wide floor in kg/m.

Figure 2 illustrates the verification of the proposed design criterion for TCC floors using the limited laboratory data and the field floor data. Each symbol represented a subjectively rated TCC floor.

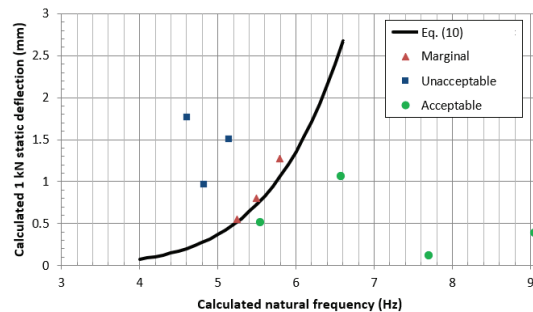


Figure 2: Verification of the proposed design criterion for controlling vibration of TCC floors

## 7 ULTIMATE LIMIT STATE DESIGN

TCC floors are made of three components: timber, concrete and shear connectors, where each of them can limit the strength of the floor. In the following section, equations are developed to evaluate the bending moment and the shear resistance of the whole TCC floors by considering the component that would fail first.

The shear connector can be 1) brittle or is not allowed to yield or 2) ductile and is allowed to yield. In these two different scenarios, the resisting equations are not the same. In the first scenario, the  $\gamma$ -method is used to estimate the force in each component. The TCC floor

design resistance is achieved when the first component achieved its ultimate resistance. The second scenario assumes that each connector has yielded which changes the equilibrium cinematic compared to the  $\gamma$ -method. Consequently, an elasto-plastic model (EPM) [28] is used to estimate the force on each component and the TCC floor ultimate resistance is achieved when the timber or the concrete achieved its ultimate resistance. It should be noted that the shear connector under serviceability load must remain in its elastic behaviour which is verified with the  $\gamma$ -method.

If the connector is ductile and the resistance of the TCC floor is limited by the  $\gamma$ -method, the floor will likely be brittle. Comparatively, if the resistance is limited by the EPM, the floor will have inelastic deformation before collapse. Figure 3 shows typical load-deflection curve of TCC floor. The  $\gamma$ -method will limit the resistance of the floor if the floor fails in the first circled portion and the EPM will limit the resistance of the floor if the floor fail in the second circled portion.

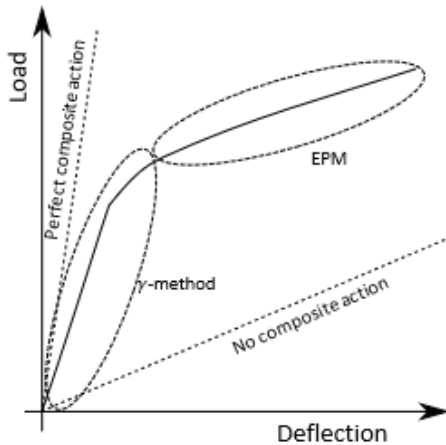


Figure 3: Failure mechanism of TCC floors

If not all the connectors have yielded when the floor fails, that situation is not directly accounted either in the  $\gamma$ -method and the EPM. However, in the  $\gamma$ -method the shear stiffness of the connectors is usually reduced when calculating the ultimate resistance of the floor which partially accounts this situation. Moreover, in the EPM the total shear load given by all the yielded connectors is estimated with their design resistance. Due to repeatability effect, the total shear load given by the connectors in the EPM gives a smaller probability of failure compared to a single shear connector. Consequently, in the design calculation, the EPM gives a conservative design value if all the connectors have yielded.

## 7.1 BENDING RESISTANCE

### 7.1.1 Gamma method

A bending moment applied on a composite floor ( $M$ ) induced a bending moment ( $M_i$ ) and an axial force ( $N_i$ ) on each layer where  $i$  is used to either represent the timber component,  $t$ , or the concrete component,  $c$ . According to

the  $\gamma$ -method, the axial force and the bending moment on each layer is calculated with the following formulae:

$$N_i = \frac{\gamma_i(EA)_i a_i}{(EI)_{eff}} M \quad (12)$$

$$M_i = \frac{(EI)_i}{(EI)_{eff}} M \quad (13)$$

The maximum axial stress on a given component is equal to the following equation:

$$\sigma_{max,i} = \frac{M}{b_i h_i (EI)_{eff}} \left( \frac{6(EI)_i}{h_i} + \gamma_i (EA)_i a_i \right) \quad (14)$$

However, for the timber element, only looking the maximum stress is not sufficient. The interaction between the axial force and the bending moment need verification with the following combined efforts interaction in accordance with CSA O86-19 [7]:

$$\frac{T_{f,t}}{T_{r,t}} + \frac{M_{f,t}}{M_{r,t}} \leq 1.0 \quad (15)$$

Where  $T_{r,t}$  and  $M_{r,t}$  are the tension and bending moment resistance, respectively, for the timber element evaluated with the CSA O86-19 [7] and  $T_{f,t}$  and  $M_{f,t}$  are the tension and bending moment force resisted by the timber component. The bending moment resistance of a TCC floor limited by the timber can be determined by substituting Equations (12) and (13) into Equation(14):

$$M_{r,\gamma,t} = \frac{(EI)_{eff} T_{r,t} M_{r,t}}{\gamma_t (EA)_t a_t M_{r,t} + (EI)_t T_{r,t}} \quad (16)$$

The bending moment resistance of a TCC floor limited by the concrete component is determined by ensuring that the maximum axial stress of the concrete does not exceed  $0.9\phi_c f'_c$  which is in consistent with CSA A23.3-19 [11]. However, ensuring that the concrete never exceeds  $0.9\phi_c f'_c$  with a triangular stress distribution is very conservative since concrete is able to have some inelastic deformation.

$$M_{r,\gamma,c} = 0.9\phi_c f'_c S_c \quad (17)$$

$$S_c = \frac{(EI)_{eff}}{E_c(0.5h_c + \gamma_c a_c)} \quad (18)$$

As a result, the bending moment resistance of a TCC floor when the shear connectors are brittle or not allowed to yield is:

$$M_{r,\gamma} = \min(M_{r,\gamma,t}; M_{r,\gamma,c}) \quad (19)$$

### 7.1.2 Elasto-plastic model

The bending moment resistance evaluated with the  $\gamma$ -method assumes that each component has a linear elastic behaviour. However, if the connector yields before failure

of the timber or the concrete element, bending moment resistance given by the  $\gamma$ -method may overestimate the resistance which is why bending moment resistance needs to be limited as a function of the connection's strength determined from the EPM ( $M_{r,EP}$ ). When calculating the resistance with the EPM, the connectors must exhibit a ductile behaviour.

To consider the ductility of the connectors, Frangi & Fontana [28] proposed a method which accounts the strength of the connectors. The principles of this method are similar to the method in CSA S16-19 [29] for calculating the bending moment resistance of a steel-concrete beam, with some minor differences. When the connectors are allowed to yield, the following equation needs to be respected:

$$M_r = \min(M_{r,\gamma,t}; M_{r,\gamma,c}; M_{r,EP}) \quad (20)$$

where  $M_{r,EP}$  is the bending moment resistance evaluated with the EPM developed by Frangi & Fontana [28] describes in this section. They developed the equations to evaluate the bending moment resistance considering that the timber fails first, while a part of the concrete is in tension, which is usually the case. However, to consider all possible scenarios, the equations for the bending resistance in the event that the concrete fails first or when the entire thickness of the concrete is in compression were also developed.

Based on the assumption that all connectors have yielded at the collapse mechanism, the maximum shear force that can be transferred to each layer is calculated from the design connector strength ( $V_{r,conn}$ ) and the number of connectors ( $m$ ) located between the critical cross-section and one point of zero moment:

$$N_c = N_t = N = mV_{r,conn} \leq \min(T_{r,t}; 0.9\phi_c f'_c A_c) \quad (21)$$

If  $mV_{r,conn} \geq \min(T_{r,t}; 0.9\phi_c f'_c A_c)$ , it means that the concrete or the timber will reach its resistance before that all the connectors have yielded. In that case,  $N = \min(T_{r,t}; 0.9\phi_c f'_c A_c)$ ,  $h_{c,eff} = h_c$ ,  $\sigma_{b,t} = \sigma_{b,c} = 0$ , when evaluating  $M_{r,EP}$  with Equation (31).

If the bending moment resistance of the composite floor is governed by the timber design strength, the bending stress applied on the timber  $\sigma_{b,t}$  is calculated as follows:

$$\sigma_{b,t} = \left(1.0 - \frac{N}{T_{r,t}}\right) \frac{6M_{r,t}}{b_t h_t^2} \quad (22)$$

If a part of the concrete is in tension,  $h_{c,eff}$  and  $\sigma_{b,c}$  are calculated as:

$$h_{c,eff} = \sqrt{\frac{NE_t h_t}{E_c \sigma_{b,t} b_c}} \leq h_c \quad (23)$$

$$\sigma_{b,c} = \frac{N}{b_c h_{c,eff}} \leq 0.45\phi_c f'_c \quad (24)$$

Note that  $E_t$  in the EPM is equal to  $12(EI)_t / (b_t h_t^3)$ . If the limitation of Equation (23) is not respected, then the entire thickness of the concrete is in compression and  $h_{c,eff} = h_c$  and  $\sigma_{b,c}$  is calculated as:

$$\sigma_{b,c} = \frac{E_c h_{c,eff}}{E_t h_t} \sigma_{b,t} \leq \left(0.9\phi_c f'_c - \frac{N}{b_c h_{c,eff}}\right) \quad (25)$$

If the limitation of Equation (24) or (25) is not respected then the bending moment resistance of the composite floor is governed by the concrete strength. If a part of the concrete is in tension,  $h_{c,eff}$ ,  $\sigma_{b,c}$  and  $\sigma_{b,t}$  are calculated as follows:

$$h_{c,eff} = \frac{2N}{0.9\phi_c f'_c b_c} \leq h_c \quad (26)$$

$$\sigma_{b,c} = 0.45\phi_c f'_c \quad (27)$$

$$\sigma_{b,t} = \frac{E_t h_t b_c (0.9\phi_c f'_c)^2}{4E_c N} \leq \left(1.0 - \frac{N}{T_{r,t}}\right) \frac{6M_{r,t}}{b_t h_t^2} \quad (28)$$

If the limitation of Equation (26) is not respected then the entire thickness of the concrete is in compression and  $h_{c,eff} = h_c$  and  $\sigma_{b,c}$  and  $\sigma_{b,t}$  are calculated as follows:

$$\sigma_{b,c} = 0.9\phi_c f'_c - \frac{N}{b_c h_{c,eff}} \leq \frac{N}{b_c h_{c,eff}} \quad (29)$$

$$\sigma_{b,t} = \frac{E_t h_t}{E_c h_c} \left(0.9\phi_c f'_c - \frac{N}{b_c h_{c,eff}}\right) \leq \left(1.0 - \frac{N}{T_{r,t}}\right) \frac{6M_{r,t}}{b_t h_t^2} \quad (30)$$

Once  $N$ ,  $h_{c,eff}$ ,  $\sigma_{b,c}$  and  $\sigma_{b,t}$  are known, the bending moment resistance of the composite floor is calculated as follows:

$$M_{r,EP} = N \left( \frac{h_t}{2} + t + h_c - \frac{h_{c,eff}}{2} \right) + \sigma_{b,c} \frac{b_c h_{c,eff}^2}{6} + \sigma_{b,t} \frac{b_t h_t^2}{6} \quad (31)$$

## 7.2 SHEAR RESISTANCE

### 7.2.1 Gamma method

The shear resistance of a TCC floor can be dictated by the strength of the connectors, the timber or the concrete. From the Eurocode 5 [10], the shear flow at the connection interface ( $\tau_{conn}$ ) is evaluated with the following formulae:

$$\tau_{conn} = \frac{\gamma_t(EA)_t a_t}{(EI)_{eff}} V \quad (32)$$

$V$  is the applied shear force on the whole TCC section. The applied shear force at one connector ( $V_{conn}$ ) is afterwards evaluated with the following equation:

$$V_{conn} = \frac{\tau_{conn} s}{n} = \frac{\gamma_t(EA)_t a_t s}{n(EI)_{eff}} V \quad (33)$$

Where  $s$  is the tributary spacing of the considered shear connector and  $n$  is the number of rows of shear connectors. Equation (33) can be rewritten to estimate the shear resistance of the whole composite floor dictated by the connection shear resistance with the  $\gamma$ -method ( $V_{r,\gamma,conn}$ ) as follows:

$$V_{r,\gamma,conn} = \frac{n(EI)_{eff}}{\gamma_t(EA)_t a_t s} V_{r,conn} \quad (34)$$

where  $V_{r,conn}$  is the design connection shear resistance.

The vertical shear stress in the timber and concrete elements according to the classical beam theory (and the theory of mechanically jointed beams [10]) is calculated as follows:

$$\tau_{max,i} = \frac{V(EQ)_i}{(EI)_{eff} b_i} \quad (35)$$

where,

$$(EQ)_i = \frac{y_i}{h_i} \left( \frac{6(EI)_i}{h_i} \left( 1 - \frac{y_i}{h_i} \right) + \gamma_i(EA)_i a_i \right) \quad (36)$$

$y_i$  is the position at which the shear stress is evaluated. Knowing that the shear stress is critical at the neutral axis evaluated as  $y_{NA,i} = h_i/2 + \gamma_i a_i$  the maximum stress within a layer is then:

$$\tau_{max,i} = \begin{cases} \frac{0.5E_i \left( \frac{h_i}{2} + \gamma_i a_i \right)^2}{(EI)_{eff}} V, & y_{NA,i} < h_i \\ \frac{E_i h_i \gamma_i a_i}{(EI)_{eff}} V, & y_{NA,i} \geq h_i \end{cases} \quad (37)$$

If there is no neutral axis in the layer, the shear stress is maximal at the interface, as dictated from the second expression in Equation (37).

In Canada, the verification according to design standard is based on the force instead of the stress. According to the theory of mechanically jointed beams, the shear force in each component is calculated with the following equation:

$$V_i = \frac{(EI)_i + 0.5\gamma_i(EA)_i h_i a_i}{(EI)_{eff}} V \quad (38)$$

Equation (38) can be rewritten to estimate the shear resistance of the whole composite floor dictated by the timber shear resistance or the concrete shear resistance with the  $\gamma$ -method as follows:

$$V_{r,\gamma,t} = \frac{(EI)_{eff}}{(EI)_t + 0.5\gamma_t(EA)_t (h_t + t) a_t} V_{r,t} \quad (39)$$

$$V_{r,\gamma,c} = \frac{(EI)_{eff}}{(EI)_c + 0.5\gamma_c(EA)_c (2h_c - h_{c,eff} + t) a_c} V_{r,c} \quad (40)$$

where  $V_{r,t}$  is the design shear resistance of the timber component and  $V_{r,c}$  is the design shear resistance of the concrete slab. It must be noted that in Equations (39) and (40) the gap,  $t$ , have been added in the equation to ensure that the total vertical shear force can be resisted by the concrete and the timber component.

The shear resistance of the whole TCC floors is reached when the first component reaches its strength. Thus, the following equation gives the shear resistance of the whole TCC floors ( $V_{r,\gamma}$ ).

$$V_r = \min(V_{r,\gamma,conn}; V_{r,\gamma,t}; V_{r,\gamma,c}) \quad (41)$$

If the connector resistance is reached before the shear resistance of the timber or the concrete, that doesn't necessarily mean failure of the TCC floor if the connectors exhibit a ductile behaviour [28,30,31]. When the capacity of the ductile shear connector is reached, it will transfer its forces to the concrete and timber elements until one of them fail. As a conservative design, Equation (41) may be used to evaluate the shear resistance of the TCC floor when the connector is ductile. However, if the designer wants to benefit on the ductility of the connector, the following equation can be used:

$$V_r = \min(V_{r,\gamma,t}; V_{r,\gamma,c}; V_{r,EP,t}; V_{r,EP,c}) \quad (42)$$

where  $V_{r,EP}$  is the shear resistance following the EPM. Although the shear connectors are ductile, the shear resistance limited by the shear connector,  $V_{r,\gamma,conn}$ , must be higher than the serviceability shear load in order to limit the fatigue phenomena and ensuring accuracy in the deflection calculation.

### 7.2.2 Elasto-plastic model

More details for the shear resistance calculated with the EPM is given in the design guide for TCC floors in Canada written by FPInnovations [8].

## 8 STRUCTURAL FIRE-RESISTANCE

This section addresses the structural fire-resistance of a TCC floors subjected to a standard fire from underneath and does not address all the other subjects related to the

fire safety, such as the separating function of floor assemblies. In order to develop and validate a calculation method to predict the time of structural fire-resistance for a TCC floor, FPInnovations [32, 33] tested three different TCC floors exposed to a standard fire such as that specified in CAN/ULC-S101 and ASTM E119. The span of these three floors was 4815 mm with an applied live load of 2.4 kPa. One of the floors consisted of a series of nine screw-laminated 2x8 “beams” (38 x 184 mm, on the edge), where each build-up beams consisted of five pieces of lumber boards. Conventional truss plates were used as shear connectors into 89 mm reinforced concrete as shown in Figure 4a. A second floor consisted of a 5-ply (175 mm) E1 stress grade CLT and 89 mm concrete, connected using self-tapping screws driven at 45° into the CLT, as shown in Figure 4b. The third floor consisted of 5¼” x 16” (133 x 406 mm, on flat) laminated veneer lumber (LVL). Lag screws were used as shear connectors, as shown in Figure 4c, to 89 mm concrete topping. All of these floors were fully exposed to the standard fire from underneath (i.e. timber components were exposed to fire).



**Figure 4:** TCC floors under construction for fire-resistance testing

Based on the data gathered from the tested TCC floors exposed to the CAN/ULC S101 standard fire, it was found that the shear connectors have little to no impact on the heat transfer into the assembly. Even the lag screws’ larger diameter did not create a significant increase in heat transfer through the assembly as the shear connector becomes exposed to fire from underneath. Consequently, as long as the connector is not exposed to fire (i.e., remains in the reduced timber cross-section), it can be assumed that the shear resistance and the shear stiffness of the connector are not affected. However, when the timber element is exposed to fire on its side and underneath (e.g. timber beam), the wood that covers the shear connector on the side must be at least 35 mm to remain thermally thick (i.e. to limit heat transfer up to the connector). When the wood cover is less than 35 mm, the temperature into the connection can increase significantly and then greatly affect its mechanical properties.

When the connector becomes exposed to fire from underneath, its shear resistance should be estimated using the appropriate design provisions as a function of its residual penetration depth into the timber. If it is not possible to estimate the shear resistance with those design provisions, its strength may be reduced proportionally to its remaining depth. This design assumption may not be applicable for all shear connectors. Consequently, applying this assumption is at the judgment of the structural engineer of record.

When no test data are available, the reduced shear stiffness of the shear connector could be proportional to the loss of strength. This assumption may not be applicable for all shear connectors, but has been validated with self-tapping screws inserted with an angle of 45°, lag screws and truss plates in the following references [32, 33]. It is at the judgment of the structural engineer of record to apply or not this hypothesis in function of the shear connector.

Table 1 gives the structural failure times obtained from these three tested floors and those predicted using the methodology proposed herein.

**Table 1:** Fire-resistance of TCC floors – Test data vs. calculation method

	NLT- Concrete	CLT- Concrete	LVL- Concrete
Shear connector	Truss plate	Self-tapping screws	Lag screws
Test failure time (min)	>214*	214	191
Predicted failure time	247	198**	165

\*Test was stopped when the CLT-concrete floor failed. No failure was reached for the NLT-concrete floor.

\*\*Using the effective charring model from Annex B of CSA O86-19 [7]

The predicted structural fire-resistance failure times are calculated using laboratory shear connector test results (stiffness and resistance). The shear connector properties were proportionally reduced linearly as a function of its remaining penetration depth once it was exposed to fire. The predicted times are conservative for the CLT-concrete and LVL-concrete composite floors. For the NLT-concrete floor, the predicted failure time seems realistic, but it is uncertain whether the estimation is conservative, or not, since the test was stopped after 214 min; time at which the CLT-concrete floor failed first (CLT and NLT were tested simultaneously in the same furnace).

Figure 5 shows the predicted deflection as a function of time for the LVL-concrete composite floor with two different assumptions. One predicted curve assumes that the stiffness of the connectors is reduced proportionally to its remaining penetration depth and the other curve uses the stiffness of the connectors based on shear test results conducted at different remaining penetration depths into

the LVL. The deflection was estimated by reducing the thickness of the wood through time and the shear connector stiffness which impacted the calculated  $(EI)_{eff}$ . For the LVL-concrete composite floor with lag screws as shear connectors, the estimated deflection and residual resistance are conservative when assuming that the properties of the shear connector are reduced proportionally to its remaining penetration depth. The predicted deflection is also quite accurate when compared to the experimental results using shear connector properties being modified based on experimental shear test results.

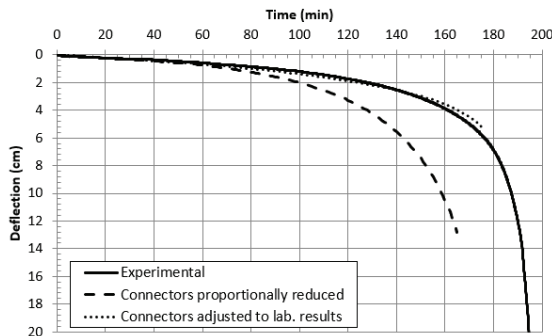


**Figure 5:** Comparison between the experimental and the predicted deflections in function of time curves

From these tests, it is concluded that when the composite floor is made with a timber slab (bottom), the timber effectively protects the concrete (top) from the thermal effects from fire underneath. Consequently, the strength of the TCC slab floor can be calculated by simply reducing the timber cross-section due to charring and the connector properties as a function of its remaining penetration depth. However, when the floor is made with timber beams instead of a timber slab, the concrete located between beams becomes fully exposed to fire and its fire resistance shall be calculated in accordance with the applicable design provisions found in the NBC [34].

## 9 CONCLUSIONS

With the information currently available in the literature and laboratory test results, FPInnovations developed a design guide for timber-concrete composite floors with a focus on the Canadian design code. This paper presents a summary of this design method.

At the time of writing this paper, design provisions were developed for implementations in the next 2024 edition of CSA O86. The methodology presented in the technical guide was used to develop the provisions, which have been slightly modified based on CSA O86 Task Group members. Limitations are also proposed, such as simple span TCC floors and TCC floors consisted of slab elements only.

## ACKNOWLEDGEMENT

FPInnovations would like to thank its industry members and Natural Resources Canada (Canadian Forest Service) for their financial supports of this work.

## REFERENCES

- [1] A. Ceccotti, "Composite concrete-timber structures," *Progress in Structural Engineering and Materials*, vol. 4, no. 3, pp. 264-275, 2002.
- [2] P. Mueller, "Decke aus hochkantig stehenden Holzbohlen oder Holzbrettern und Betondeckschicht". 1921.
- [3] O. Schaub, "Wood reinforced concrete structural member". 1931.
- [4] F. E. Richart and C. B. Williams, "Tests of composite timber and concrete beams," *University of Illinois bulletin*, vol. 40, no. 38, 1943.
- [5] J. N. Rodrigues, A. M. P. G. Dias and P. Providência, "Timber-concrete composite bridges: state-of-the-art review," *BioResources*, vol. 8, no. 4, pp. 6630-6649, 2013.
- [6] D. Yeoh, M. Fragiaco, M. De Franceschi and K. Heng Boon, "State of the art on timber-concrete composite structures: Literature review," *Journal of structural engineering*, vol. 137, no. 10, pp. 1085-1095, 2010.
- [7] CSA O86-19, Engineering design in wood, Mississauga, Ontario, Canada: Canadian standard association, 2019.
- [8] S. Cuerrier-Auclair, "Design Guide for Timber-Concrete Composite Floors in Canada : Special Publication SP-540E," FPInnovations, Pointe-Claire, Qc, Canada, 2020.
- [9] K. Möhler, Über das Tragverhalten von Biegeträgern und Druckstäben mit zusammengesetzten Querschnitten und nachgiebigen Verbindungsmitteln, Karlsruhe, 1956.
- [10] European Committee for Standardization (CEN), Eurocode 5 - Design of timber structures - Part 1-1: General rules and rules for buildings (EN 1995-1-1:2004+A1:2008), 2008.
- [11] CSA A23.3-19, Design of concrete structures, Mississauga, Ontario, Canada: Canadian standard association, 2019.
- [12] A. Dias, S. Lopes, J. Van de Kuilen and H. Cruz, "Load-carrying capacity of timber concrete joints with dowel-type fasteners," *Journal of Structural Engineering*, vol. 133, no. 5, pp. 720-727, 2007.
- [13] A. Dias, U. Kuhlmann, K. Kudla and S. Mönch, "Performance of dowel-type fasteners and notches for hybrid timber structures," *Engineering Structures*, vol. 171, pp. 40-46, 2018.
- [14] M. Derikvand and G. Fink, "Deconstructable connector for TCC floors using self-tapping screws," *Journal of Building Engineering*, vol. 42, 2021.
- [15] P. Clouston and A. Schreyer, "Design and use of wood-concrete composites," *Practice Periodical on Structural Design and Construction*, vol. 4, no. 13, pp. 167-174, 2008.



- [16] S. Cuerrier-Auclair, L. Sorelli and A. Salenikovich, "A new composite connector for timber concrete composite structures," *Construction and Building Materials*, vol. 112, pp. 84-92, 2016.
- [17] M. Brunner, M. Romer and M. Schnüriger, "Timber-concrete-composite with an adhesive connector (wet on wet process)," *Materials and Structures*, vol. 40, pp. 119-126, 2007.
- [18] D. Yeoh, M. Fragiaco, M. De Franceschi and A. Buchanan, "Experimental Tests of Notched and Plate Connectors for LVL-Concrete Composite Beams," *Journal of Structural Engineering*, vol. 137, no. 2, 2011.
- [19] M. Shahnewaz, R. Jackson and T. Tannert, "CLT concrete composite floors with steel kerf plate connectors," *Construction and Building Materials*, vol. 319, 2022.
- [20] International Organisation for Standardization, ISO 6891:1983, Timber structures — Joints made with mechanical fasteners — General principles for the determination of strength and deformation characteristics, Geneva, 1983.
- [21] J. H. Rainer and G. Pernica, Vertical dynamic forces from footsteps, Ottawa: National Research Council Canada, 1986.
- [22] S. V. Ohlsson, "Serviceability criteria - especially floor vibration criteria," *Proceedings of 1991 International Timber Engineering Conference*, pp. 58-65, September 1991.
- [23] A. Ebrahimpour, R. L. Sack, W. N. Patten and A. Hamam, "Experimental measurements of dynamic loads imposed by moving crowds," *Structures Congress XII*, pp. 1385-1390, 1994.
- [24] S. C. Kerr and N. W. M. Bishop, "Human induced loading on flexible staircases," *Engineering Structures*, vol. 23, no. 1, pp. 37-45, 2001.
- [25] International Organisation for Standardization, ISO 18324:2016, Timber structures -- Test methods -- Floor vibration performance, Geneva, 2016.
- [26] International Organisation for Standardization, ISO 21136:2017, Timber structures -- Vibration performance criteria for timber floors, Geneva, 2017.
- [27] S. Cuerrier-Auclair, L. Hu and R. Ramzi, "Design method for vibration control of timber-concrete composite floor," FPInnovations, 2018.
- [28] A. Frangi and M. Fontana, "Elasto-plastic model for timber-concrete composite beams with ductile connection," *Structural Engineering International*, vol. 13, no. 1, pp. 47-57, 2003.
- [29] CSA S16-19, Design of steel structures, Mississauga, Ontario, Canada: Canadian Standards Association, 2019.
- [30] S. Cuerrier-Auclair, L. Sorelli and A. Salenikovich, "Simplified nonlinear model for timber-concrete composite beams," *International Journal of Mechanical Sciences*, vol. 117, pp. 30-42, 2016.
- [31] A. M. Dias and L. F. Jorge, "The effect of ductile connectors on the behaviour of timber-concrete composite beams," *Engineering Structures*, vol. 33, no. 11, pp. 3033-3042, 2011.
- [32] L. Osborne, «Fire Resistance of Long Span Composite Wood-Concrete Floor Systems (Project No. 301009649),» FPInnovations, 2015.
- [33] L. Ranger, C. Dagenais and S. C.-Auclair, Fire-resistance of timber-concrete composite floor using laminated veneer lumber, Project Report No. 301010618, FPInnovations, 2016.
- [34] Canadian Commission on Building and Fire Codes, "National Building Code of Canada: 2020," National Research Council of Canada, 2022.